

## Understanding and improving the subsalt image at Thunder Horse, Gulf of Mexico

Ken Hartman<sup>1</sup>, Samarjit Chakraborty<sup>1</sup>, Bertram Nolte<sup>1</sup>, Weiping Gou<sup>\*2</sup>, Qingqing Sun<sup>2</sup>, Nicolas Chazalnoel<sup>2</sup>

<sup>1</sup>BP

<sup>2</sup>CGG

### Summary

Subsalt imaging at the Thunder Horse Field in the Gulf of Mexico is challenging primarily because the salt canopy, overlying roughly 75% of the structure, greatly distorts subsalt illumination and causes imaging and resolution problems. Since the Thunder Horse discovery, advancements in seismic acquisition techniques and imaging technologies have significantly improved subsalt images. The latest successful application is from a tilted transverse isotropy (TTI) reverse time migration (RTM) project combining two wide azimuth towed streamer (WATS) data sets and three narrow azimuth towed streamer (NATS) data sets. The addition of an extra WATS data set and the application of the recent imaging technologies are key contributors to the dramatic structural image improvements with better defined three-way events and a higher signal-to-noise ratio (S/N).

### Introduction

The Thunder Horse Field has been producing since 2008 and is located in the south-central part of the Mississippi Canyon protraction area in the Gulf of Mexico. A large overlying allochthonous salt body causes rapid spatial and temporal changes in illumination and image quality, making interpretation difficult, especially near the steeply dipping three-way closure against the salt stock. During the course of discovery and development, BP has made continuous efforts to better understand and improve Thunder Horse's subsalt image with new seismic data sets and more advanced imaging technologies (Pfau et al., 2002; Ray et al., 2002, 2005; Gherasim et al., 2012). The latest successful TTI RTM project with two WATS data sets and three NATS data sets is the continuation of this effort to improve Thunder Horse subsalt images.

This project aimed to improve the structural image in poorly illuminated areas and to maximize the usable vertical and horizontal resolution for well targeting and planning. The latest image shows a dramatic improvement over the previous TTI RTM image produced in the 2012 project for three reasons. First, the additional WATS data in the NE-SW direction illuminated some key areas that the NW-SE WATS and three NATS surveys did not. Second, the majority of the NATS traces were migrated rather than just used to infill missing traces in the NW-SE WATS shot gathers, as was done in 2012. Finally, more advanced imaging workflows and technologies were used to address specific problem areas in the data. Shot patch-based angle

gather illumination weighting (AGILW) and input data selection technologies, which were applied in this project, effectively attenuate noise while preserving signal. Specular imaging using RTM dip gathers also helped enhance the S/N. We also discovered one of the reasons for frequency loss underneath the salt.

### Input Data Sets

The input data sets for this project included two WATS surveys acquired in the NE-SW and NW-SE directions and three NATS surveys in N-S, E-W, and NE-SW directions. The combination of these surveys provided nearly full azimuth (FAZ) coverage (Figure 1b). This contrasts with the 2012 project for which the NE-SW WATS data were not available, and the surface azimuth coverage was less complete (Figure 1a). The wider surface-azimuth coverage provided the necessary constraints for anisotropic parameter estimation (Huang et al., 2008) and resulted in a better TTI velocity model.

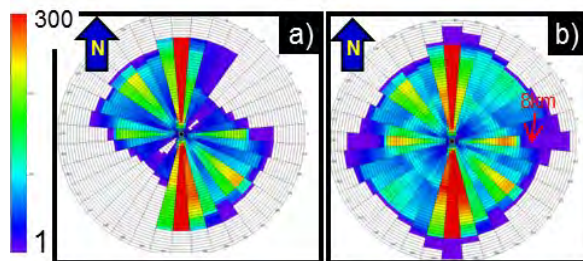


Figure 1: Rose diagram of (a) 2012 project and (b) recent project.

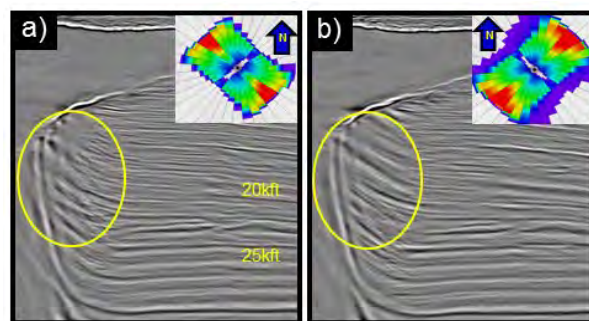


Figure 2: Vector offset output (VOO) optimized stack with (a) NW-SE WATS and (b) NE-SW WATS data. The insets show the Rose diagram of the corresponding migration input data set.

Besides providing better constraints for the TTI velocity model, the additional NE-SW WATS data was beneficial

## Improving Thunder Horse subsalt image

for illuminating some key areas that the NW-SE WATS data did not, such as a portion of the three-way closure against the salt stock. To examine this, we performed a vector offset output (VOO) RTM migration (Xu et al., 2011) with the same model but using the two different WATS data sets; identical post-migration processing techniques were applied to both. Figure 2 shows that the NE-SW WATS data set produced a considerably better three-way image than the NW-SE data set. Because the NE-SW surface data set did not exist at the time of the 2012 project, the NATS data was used as infill for the NW-SE WATS data set, and the final image had insufficient subsalt illumination at the three-way closure.

### Shot Patch-based Illumination Weighting

To further improve the S/N in the Thunder Horse subsalt area, we applied a shot patch-based AGILW scheme. The scheme is an extended version of the illumination compensation approach (Gherasim et al., 2010, 2012, and 2014), which was successfully applied in the previous Thunder Horse project and improved the subsalt image. Different from previous implementations of AGILW, our approach introduces the shot-patch concept as an additional action to further separate signal and noise. Instead of stacking the migration of all shots in a survey to form one set of image gathers, we partitioned shots into smaller shot patches and kept the migration gathers separate for each shot patch. We performed the same actions in parallel for both field and synthetic data. After that, we estimated weighting scalars from each synthetic gather for its shot patch and applied them to the field gathers of the corresponding shot patch. By doing this, we limited the cross-talk between the signal and noise coming from different shot patches; thus, the shot patch-based AGILW more effectively enhanced signal and attenuated noise compared to the original AGILW.

Our method uses the single-patch application described by Shen et al. (2011). We used RTM 3D angle domain common image gathers (ADCIGs), which were generated by a local wave-field decomposition before applying the imaging condition (Xu et al., 2011). The workflow of the shot patch-based AGILW is:

- 1) For each shot patch, produce field data RTM 3D ADCIGs  $R(x, \theta, \phi, sp)$ , where  $x$  is the imaging location,  $\theta$  is the reflection angle,  $\phi$  is the azimuth, and  $sp$  is the shot patch number.
- 2) Sum over all angles and shot patches to generate the stacked image.
- 3) Interpret target horizons on the stacked image, and create a reflector model.
- 4) Generate synthetic traces without free-surface multiples at real data locations using acoustic wave-

equation modeling with the velocity model and the reflector model.

- 5) For each shot patch of the synthetic data, produce RTM 3D ADCIGs in the same way as field data using the velocity model.
- 6) Extract the amplitude and create illumination weighting scalars  $S(x, \theta, \phi, sp)$  for each shot patch from the synthetic angle gathers.
- 7) Apply the illumination scalars to the real angle gathers, and generate the stacked image:  $I(x) = \sum S(x, \theta, \phi, sp) * R(x, \theta, \phi, sp)$ .

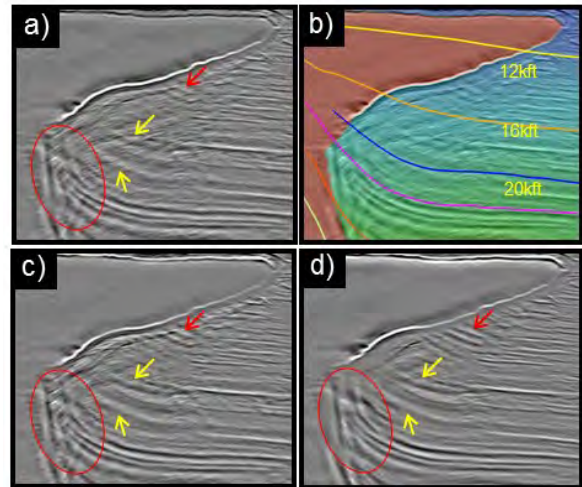


Figure 3: (a) Raw stack image. (b) Velocity model and interpretation horizons overlaid on image. (c) Original angle gather illumination weighting (AGILW) stack image. (d) Shot patch-based AGILW stack image.

We applied both the original and shot patch-based AGILW approaches to the data (Figures 3c and 3d, respectively). Compared to the raw RTM image (Figure 3a), the three-way events became cleaner and more visible after illumination compensation (indicated by the yellow arrows). Compared to the original approach, the shot patch-based approach further attenuated noise, especially converted wave noise, and produced an even cleaner three-way image that was easier to interpret (indicated by the red arrow and circle).

### Input Data-selection RTM

Full-azimuth input data sets in this project provided a better probability of imaging difficult Thunder Horse subsalt areas, especially the three-way closure against salt. However, even with FAZ geometry, some subsalt reflectors were illuminated only by small ranges of subsurface azimuths or reflection angles. Coherent noise such as mode-converted waves, residual multiples, and migration swings can easily be 20 dB stronger than the subsalt

## Improving Thunder Horse subsalt image

signals. In these cases, without proper processing, more data do not guarantee a better image. In this project, we applied an input data-selection workflow based on 3D ray-tracing to improve the RTM image in Thunder Horse three-way areas of poor illumination and low S/N.

The workflow for input data-selection RTM can be divided into the following six steps:

- 1) Use a salt body velocity model to produce an RTM stack image with all of the data.
- 2) Interpret target horizons based on the full input RTM image in the area of interest.
- 3) Run 3D ray-tracing using the same velocity model to obtain all the successful rays (shot/receiver pairs) illuminating this target horizon
- 4) Generate illumination QC products (e.g., shot fold map, reflector hit map, Rose diagram).
- 5) Use the information from Step 4 to select a portion of the data (on both the shot and receiver sides) that contributes to the target reflector for migration.
- 6) Migrate the selected data, and merge the output volume into the full migration.

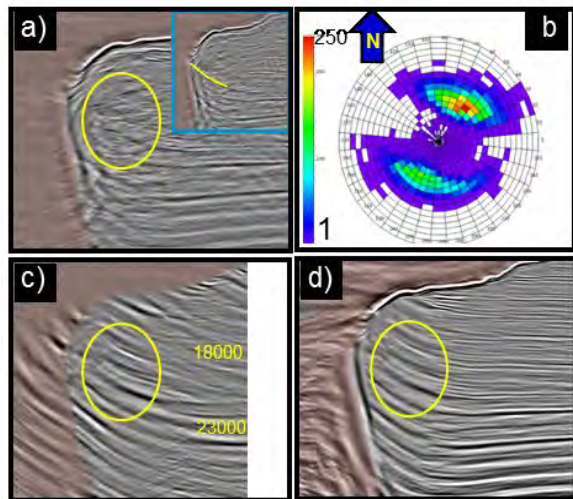


Figure 4: (a) Full input raw reverse time migration (RTM) image. Yellow line overlying the inset image shows the target horizon for the input data selection. (b) Rose diagram for selected input data. (c) Input selection RTM migration. (d) Final merged image that incorporates input selection migration to VOO optimized stack at three-way closure.

We applied the input data selection flow to the three-way closure area where the S/N was generally poor on the full input RTM image (Figure 4a). We interpreted horizons on this RTM image (Figure 4a, inset) and performed the data selection procedure. The Rose diagram generated from selective input (Figure 4b) indicated that most of illumination of this target three-way event originated from the middle offsets of NE-SW data set, which was not

available in the 2012 project. This also confirmed the benefit of the additional NE-SW WATS data set in the current project. The input data selection migration (Figure 4c) showed a much cleaner three-way image at the target horizon, which was easier to interpret compared to the raw RTM image (Figure 4a, yellow circle). We generated the final merged stack image by incorporating the selective migration into the optimized VOO stack image (Figure 4d).

### RTM Dip Gathers

As a separate product, RTM 3D dip gathers were used as a specular imaging tool to attenuate noise and enhance the subsalt image. The RTM dip gathers were generated by the directional wavefield decomposition among dip and azimuth angles at each image point (Li et al., 2012; Xu et al., 2011). In dip gathers, each dip-azimuth angle pair represents a possible subsurface structure. An optimized stack image can be generated by stacking dipoles that better conform to prior knowledge of the subsalt structure.

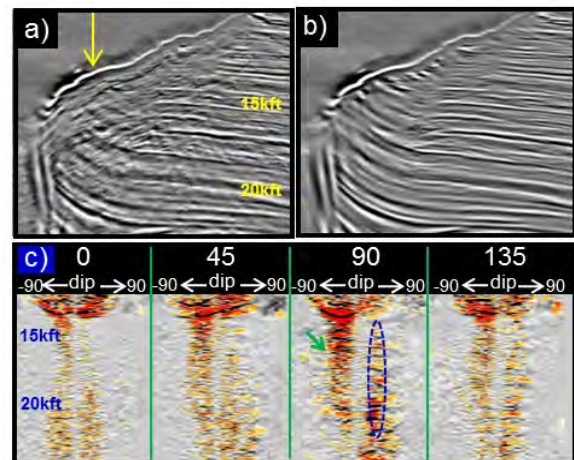


Figure 5: (a) Raw RTM stacked image from all dip angles. (b) Optimized stacked image from selective dip angles. (c) Dip gather at the location indicated by yellow arrow on (a) with 0, 45, 90, and 135 degree azimuths and a dip angle from -90 to 90 degrees.

The raw stacked image (Figure 5a) was very noisy at the subsalt three-way closure area and was heavily contaminated by converted wave noise. Viewing the dip gathers (Figure 5c) at the location indicated by the yellow arrow in Figure 5a showed that signal in the blue oval and converted wave noise at the green arrow were well separated. Therefore, attenuating noise in the dip gather domain was straightforward. With an interpretation guide, we obtained an optimized image (Figure 5b) by assigning weights to each dip angle based on the consistency between the dip in the interpretation and the dip in the gathers. Because dipoles from noise energy were excluded, a cleaner image was produced with a substantially improved S/N.

## Improving Thunder Horse subsalt image

### Image Comparisons and Discussion

We produced three main final products: an optimized RTM VOO stack incorporating the input selection image, a shot patch-based AGILW image, and an optimized stack image from RTM dip gathers. Each image had its own benefit locally, and they were all better than the final image from the 2012 processing. The final image (Figure 6b) was generated by optimized stacking of the three images based on semblance and coherency. Compared to the image from the 2012 project (Figure 6a), our final image had an improved structural image quality with better defined three-way events and a higher S/N. Although the addition of the new WATS data may have made a respectable impact on its own, it was the application of this new suite of imaging enhancement techniques that fully unleashed our imaging capabilities with the new data set.

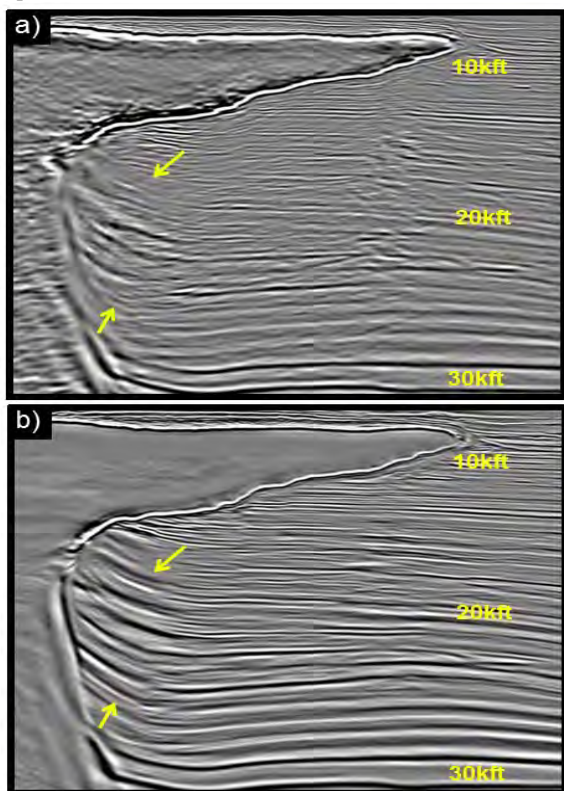


Figure 6: Final image of (a) 2012 project and (b) the recent project.

During the project, we discovered an important fact about the frequency loss underneath the salt canopy. Figure 7a shows how the frequency content of the data changed from high to low frequency with closer proximity to the salt stock. To understand this phenomenon, we performed a data-selection flow based on 3D ray-tracing for the target events (Figure 7a, green and yellow lines) and then generated Rose diagrams (Figure 7b for the yellow target;

Figure 7c for the green target). The Rose diagrams showed that all offsets contributed to the higher frequency area; however, mainly the middle and far offsets contributed to the low-frequency area. This frequency change was likely due to an illumination pattern change. Because of the missing near offset contribution and the migration stretching effect from the far offset, the area near to the salt naturally appeared to have a lower frequency. To further improve the image resolution at this area, new acquisition techniques might be needed, such as vertical seismic profile data, which records near offset energy missing from surface data at three-way areas.

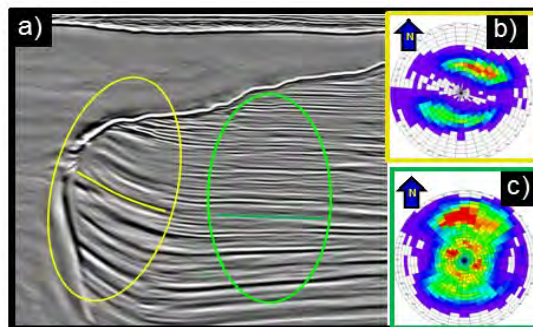


Figure 7: (a) RTM image of a key area. The yellow circle indicates the lower frequency, and the green circle indicates the higher frequency. Rose diagrams of selected data for a target event indicated by the (b) yellow and (c) green lines with a 9 km offset.

### Conclusions

The recent TTI processing at the Thunder Horse Field greatly improved the structural image in poorly illuminated areas. The dramatic improvement over the 2012 TTI RTM image mainly resulted from additional NE-SW data, better use of existing data, and the application of recent technologies. Shot patch-based AGILW, input data selection migration, and dip gather optimized stacks worked effectively to attenuate noise and improve the Thunder Horse subsalt image. We also learned that the frequency loss underneath the salt in some key areas was closely related to the missing near offset contribution and the migration stretching effect on far offset data, which was already impacting future acquisition and processing plans.

### Acknowledgements

We thank BP, ExxonMobil, and CGG for permission to present this work. We thank TGS for permission to show their data sets. We are also very grateful to Gary Murphy for his input and fruitful discussions over the course of the project.

Finally we also thank the subsurface team members of all these companies for their valuable feedback and contributions to this project.

## EDITED REFERENCES

Note: This reference list is a copyedited version of the reference list submitted by the author. Reference lists for the 2015 SEG Technical Program Expanded Abstracts have been copyedited so that references provided with the online metadata for each paper will achieve a high degree of linking to cited sources that appear on the Web.

## REFERENCES

- Gherasim, M., U. Albertin, B. Nolte, and O. J. Askim, 2010, Wave-equation angle-based illumination weighting for optimized subsalt imaging: 80th Annual International Meeting, SEG, Expanded Abstracts, 3293–3297.
- Gherasim, M., U. Albertin, B. Nolte, J. Etgen, P. Vu, P. Jilek, M. Trout, and K. Hartman, 2012, Wave-equation angle-based illumination weighting study: Thunder Horse, Gulf of Mexico: 82nd Annual International Meeting, SEG, Expanded Abstracts, doi:10.1190/segam2012-0183.1.
- Gherasim, M., B. Nolte, J. Etgen, P. Jilek, P. Vu, M. Trout, and K. Hartman, 2014, Wave-equation angle-based illumination weighting for optimized subsalt images: The Leading Edge, **33**, 392–399, <http://dx.doi.org/10.1190/tle33040392.1>.
- Huang, T., S. Xu, J. Wang, G. Ionescu, and M. Richardson, 2008, The benefit of TTI tomography for dual azimuth data in Gulf of Mexico: 78th Annual International Meeting, SEG, Expanded Abstracts, 222–226.
- Li, Z., B. Tang, and S. Ji, 2012, Subsalt illumination analysis using RTM 3D dip gathers: 82nd Annual International Meeting, SEG, Expanded Abstracts, doi:10.1190/segam2012-1348.1.
- Pfau, G., R. Chen, A. Ray, J. Kapoor, B. Koechner, and U. Albertin, 2002, Imaging at Thunder Horse: 72nd Annual International Meeting, SEG, Expanded Abstracts, 432–433.
- Ray, A., G. Pfau, and R. Chen, 2002, Raytrace modeling helped in the discovery of Thunder Horse North field in the Gulf of Mexico: 72nd Annual International Meeting, SEG, Expanded Abstracts, 465–467.
- Ray, A., Y. Quist, Z. Yu, H. Sugianto, and B. Hornby, 2005, Acquisition of 2D walkaway VSP data to provide improved imaging of the Thunder Horse North field, Gulf of Mexico: 75th Annual International Meeting, SEG, Expanded Abstracts, 476–480.
- Shen, H., S. Mothi, and U. Albertin, 2011, Improving subsalt imaging with illumination-based weighting of RTM 3D angle gathers: 81st Annual International Meeting, SEG, Expanded Abstracts, 3206–3211.
- Xu, Q., Y. Li, X. Yu, and Y. Huang, 2011, Reverse time migration using vector offset output to improve sub-salt imaging — A case study at the Walker Ridge GOM: 81st Annual International Meeting, SEG, Expanded Abstracts, 3269–3274.
- Xu, S., Y. Zhang, and B. Tang, 2011, 3D angle gathers from reverse time migration: *Geophysics*, **76**, no. 2, S77–S92, <http://dx.doi.org/10.1190/1.3536527>.